

PAPER

A sensitivity correction method for a three-dimensional sound intensity probe

Hideo Suzuki, Shun Oguro, and Takahiko Ono

Ono Sokki Co., Ltd.,

1-16-1, Hakusan, Midori-ku, Yokohama, 226-8507 Japan

E-mail : suzuki@onosokki.co.jp

(Received 28 December 1999)

The upper frequency limit of a p-p type sound intensity probe is mostly determined by the sensitivity reduction of the probe. The sensitivity reduction is caused by obtaining the pressure from the average of the two pressure signals including the phase, and by obtaining the particle velocity from the finite difference of the two pressure signals. This is a systematic error suggesting a possibility of correction. In order to compensate or correct the sensitivity reduction, the direction of energy flow must be known. If a one-dimensional intensity probe is used, the probe direction must be varied to find the direction of the energy flow. If a three-dimensional intensity probe is used, the direction of the energy flow can be at least roughly estimated from a single measurement and then the sensitivity reduction can be corrected. This paper proposes a method of sensitivity reduction correction in the high frequency region for a three-dimensional (3-D) intensity probe. A theory of the method is described first and the numerical results that validate the theory will be given. This method works even for a probe with some amount of phase mismatch among microphones and for a sound field with reflections.

Keywords: Sound intensity, Probe, Three-dimensional, Sensitivity

PACS number: 43.58.-e, 43.60.-c

1. INTRODUCTION

A microphone separation of a p-p probe for the intensity measurement is determined by two reasons. It cannot be too small because of the measurement error in the low frequency region due to the phase mismatch of the microphone pair. Also, it cannot be too large because of the sensitivity reduction in the high frequency region. Sound intensity probes with microphone separations of 50 mm, 12 mm, and 6 mm are commonly used for the frequency regions of 50 Hz-1.2 kHz, 200 Hz-5 kHz, and 400 Hz-10 kHz, respectively. At each upper-frequency limits, the sensitivity of the probe decreases by approximately 1 dB.

A degree of the sensitivity reduction is known theoretically. This fact indicates a possibility of

the sensitivity correction in the high frequency region. In order to compensate the sensitivity reduction, the direction of the energy flow must be known. If a one-dimensional intensity probe is used, the probe direction must be varied to find the direction of the energy flow. If a three-dimensional intensity probe is used, the direction of the energy flow can be at least roughly estimated from the measurement and, then, the sensitivity reduction can be corrected. This paper proposes a method of sensitivity reduction correction in the high frequency region for a three-dimensional (3-D) intensity probe. A theory of the method is described first and then numerical results that validate the theory will be given.

2. SOUND INTENSITY MEASUREMENT ERROR IN THE HIGH FREQUENCY REGION

A formula used for the sound intensity measurement by the cross-spectrum method is given by Eq. (1).¹⁾

$$I(f) = -\text{Im}[G_{12}(f)]/2\pi f \rho d \quad (1)$$

where $I(f)$ is the time-averaged sound intensity as a function of frequency f , $\text{Im}[G_{12}(f)]$ is the imaginary part of the cross-spectrum $G_{12}(f)$ between the two pressure signals, d is the microphone separation, and ρ is the air density. In case of a sinusoidal plane wave without reflection, Eq. (1) is given by

$$I(f) = P_1 P_2 \sin(\phi) / 4\pi f \rho d \quad (2)$$

where P_1 and P_2 are the pressure amplitudes and ϕ is the phase difference between the two pressure signals. Let the incident angle of the wave with respect to the probe axis be θ . Then, Eq. (2) is rewritten as

$$I(f) = (P_1 P_2 / 2\rho c) (\cos \theta) [\sin(kd \cos \theta) / kd \cos \theta] \quad (3)$$

The term in the brackets in the above equation is a factor that represents the degree of sensitivity reduction. For the case of $\theta = 0^\circ$, $f = 1.2$ kHz, and $d = 50$ mm ($kd = 1.1$), the measured intensity is 0.9 dB lower than the true intensity (which is obtained when kd becomes infinitely small).

3. SENSITIVITY CORRECTION METHOD FOR A 1-D INTENSITY PROBE

As Eqs. (2) and (3) indicate, the measurement error in the high frequency region is predictable if the property of the sound field is known. When we use a one-dimensional (1-D) intensity probe for a sound field with a plane propagating wave, and if we assume that there is no phase mismatch between the microphones, a true intensity (in the direction of measurement) is recovered by multiplying the measured intensity by a correction factor

$$C_1(f) = \phi' / \sin(\phi') \quad (4)$$

for an arbitrary incident angle θ , where ϕ' is a measured phase difference between the two pressure signals, which is equal to the true phase difference $\phi = kd(\cos \theta)$ if there is no phase mismatch. A

usefulness of the correction factor $C_1(f)$ is limited since it can be used only for a single plane propagating wave field.

If once the direction of the sound wave propagation is known, however, the correction is possible even for a sound field with a reflected wave coming from the opposite direction. A correction factor for this case is given by

$$C_2(f) = kd \cos(\theta) / \sin(kd \cos(\theta)) \quad (5)$$

The effect of the correction factor is obvious by comparing Eqs. (3) and (5). The inverse of the sensitivity reduction factor in Eq. (3) is used as the correction factor. It is also obvious that correction factor $C_2(f)$ includes correction factor $C_1(f)$ since $\phi' = kd \cos \theta$ if there is no phase mismatch.

Figure 1 shows the original intensity given by Eq. (3) and intensities after the corrections by use of Eqs. (4) and (5) for the sound field with $\theta = 45^\circ$, $f = 1.2$ kHz, and $d = 50$ mm. The pressure amplitude of the reflected wave to the incoming wave (denoted as δ) is 0.5. The intensities are normalized to the true intensity including both the direct and reflected waves. The horizontal axis is the phase difference between the incoming and reflected waves at the point of measurement. The measured intensity is approximately -0.4 dB (thin solid line) and it is corrected to 0 dB (thick solid line) after multiplying the result by Eq. (5). Figure 1 indicates that the true intensity is perfectly recovered by multiplying $C_2(f)$ to the measured intensity (if there is no phase mismatch).

A reason why correction factor Eq. (5) works for

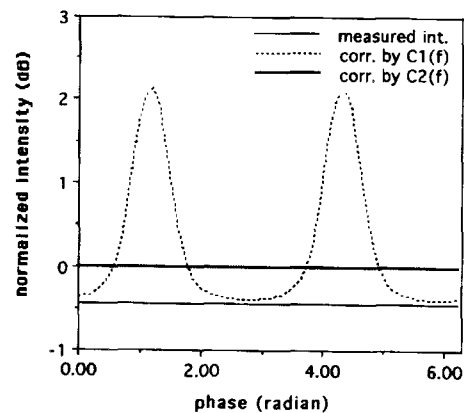


Fig. 1 Effect of corrections by $C_1(f)$ and $C_2(f)$ (solid line : original, chain line : correction by $C_1(f)$, thick solid line : correction by $C_2(f)$).

the case when the reflected wave comes from the opposite direction is understood as follows: The composed intensity is given by the sum of cross powers between the pressures and particle velocities caused by the incoming and reflected waves. The intensity generated by the incoming wave pressure and the reflected wave particle velocity has an equal amplitude but the opposite sign with the intensity generated by the reflected wave pressure and the incoming wave particle velocity. Therefore, the correction factor works simply for the incoming and reflected wave intensities, since both waves has the same incident angle to the probe.

When a 1-D probe is used, a measurement must be repeated three times with different orientations to find the direction of the wave propagation. This limits the usefulness of $C_2(f)$. This problem is solved if a 3-D intensity probe is used.

4. SENSITIVITY CORRECTION METHOD FOR A 3-D INTENSITY PROBE

A 3-D intensity probe with four microphones located at the apexes of a tetrahedron was developed (see Fig. 2).²⁾ With this intensity probe, the intensity components in the x , y , and z directions are given, respectively, by

$$\left. \begin{aligned} I_x &= -\text{Im}[G_{34} - G_{24} - 2G_{23} + G_{12} - G_{13}]/8\pi f \rho d \\ I_y &= -\text{Im}[G_{34} + G_{24} - 2G_{14} - 3G_{12} - 3G_{13}]/8\sqrt{3}\pi f \rho d \\ I_z &= \text{Im}[G_{34} + G_{24} + G_{14}]/2\sqrt{6}\pi f \rho d \end{aligned} \right\} \quad (6)$$

where d is the length of the sides of the tetrahedron and G_{ij} is the cross spectrum between the pressures at the i -th and j -th microphones. Since these equations have the same form as Eq. (1), the same idea described in section 3 is applied for the correction of the sensitivity reduction in the high frequency region. When a 3-D probe is used, the direction of the energy flow (intensity vector) is estimated from the measurement. The directional cosines between

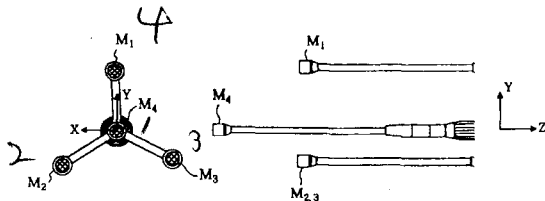


Fig. 2 Geometry of the 3-D intensity probe used for the simulation.

x , y , and z components and the estimated direction of the measured intensity I are given, respectively, by

$$\cos \alpha = I_x/I, \cos \beta = I_y/I, \cos \gamma = I_z/I \quad (7)$$

where

$$I = \sqrt{I_x^2 + I_y^2 + I_z^2} \quad (8)$$

Once α , β , and γ are obtained, the directional cosine between the estimated intensity vector and the sides of the tetrahedron determined by the i -th and j -th apexes, $\cos \theta_{ij}$, is also determined. This is given, respectively, by

$$\left. \begin{aligned} 2-4 \cos \theta_{12} &= (1/2) \cos \alpha - (\sqrt{3}/2) \cos \beta \\ 3-4 \cos \theta_{13} &= -(1/2) \cos \alpha - (\sqrt{3}/2) \cos \beta \\ 1-4 \cos \theta_{14} &= -(1/\sqrt{3}) \cos \beta - (2/\sqrt{6}) \cos \gamma \\ 2-3 \cos \theta_{23} &= -\cos \alpha \\ 1-2 \cos \theta_{24} &= -(1/2) \cos \alpha + (1/2\sqrt{3}) \cos \beta \\ &\quad - (2/\sqrt{6}) \cos \gamma \\ 1-3 \cos \theta_{34} &= (1/2) \cos \alpha + (1/2\sqrt{3}) \cos \beta \\ &\quad - (2/\sqrt{6}) \cos \gamma \end{aligned} \right\} \theta_{24} \quad (9)$$

0.2165
0.5773
0.2887

The cross spectrum G_{ij} in Eq. (6) is multiplied by the correction factor

$$C_{ij} = kd_{ij} \cos \theta_{ij} / \sin(kd_{ij} \cos \theta_{ij}) \approx 1 \quad (10)$$

where d_{ij} is the length of the side determined by the i -th and j -th apexes (which is equal to d in the present case).

The correction factor given by Eq. (10) can be used for any microphone arrangements of 3-D intensity probes as far as the cross spectral method is used.

5. NUMERICAL EVALUATION OF THE PROPOSED METHOD

The usefulness of the proposed method is evaluated numerically in this section. In a real situation, the probe may be placed with an arbitrary distance from the source. However, since the aim of this article is to evaluate the usefulness of the proposed method for a 3-D probe, the evaluation of the applicability to a field close a source and a field with multiple sources will be left as a future study.

In order to approximate a plane wave sound field, the original point source is positioned 1,000 m away from the origin of the (center of gravity of the tetrahedron). The effect of the reflection is taken into consideration by assuming an image source in the opposite direction positioned at the same distance

1 → 4
4 → 1

from the measurement point with variable source strength and phase. The direction of the source is estimated by use of Eqs. (6) and (7), and the original intensities are corrected by use of Eqs. (9) and (10).

Figure 3 shows the effect of sensitivity correction using Eq. (10) for the case with $d=60$ mm, $f=1.2$ kHz, $\delta=0.5$ (reflection ratio), $\xi=45^\circ$ and $\zeta=0^\circ$ (see Fig. 4 for the definition of the angles of the source direction). The phase errors of microphones 1 to 4 are 0° , $kd/30$, 0° , $-kd/30$, respectively ($kd/30$ is equal to 2.5°). The horizontal axis of Fig. 3 is the same as in Fig. 1. I_x and I_z are x and z components before correction and I_x' and I_z' are those after the

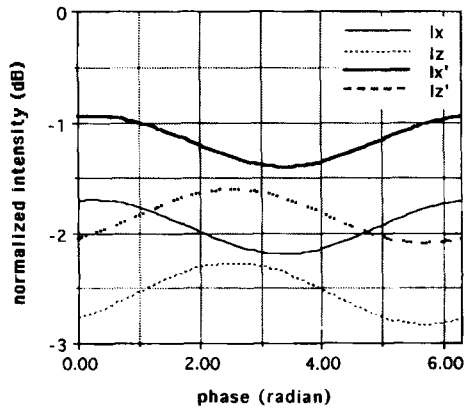


Fig. 3 Normalized intensities I_x and I_z before and after the correction shown as a function of phase difference between the primary and reflected waves ($d=60$ mm, $f=1.2$ kHz, $\delta=0.5$, $\xi=45^\circ$ and $\zeta=0^\circ$). Phase errors of microphones 1 to 4 are 0° , $+2.5^\circ$, 0° , -2.5° , respectively.

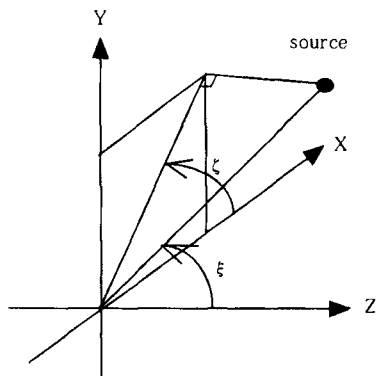


Fig. 4 Definition of the angles of the source direction.

correction. Since the direction of the source is 45° , 90° , and 45° from x , y , and z axes, respectively, the true values of the normalized intensities are $I_x=I_z=-1.5$ dB and $I_y=-\infty$ dB. If there is no phase mismatch, I_x and I_z are equal to -2.25 dB, that is, the sensitivity reduction is 0.75 dB. In the present

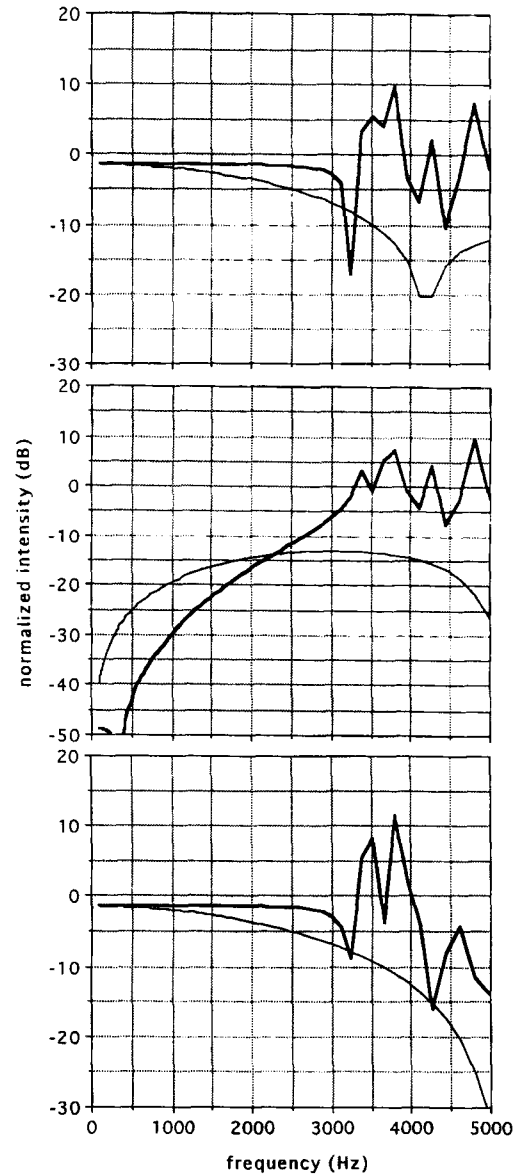


Fig. 5 Normalized intensities I_x (top), I_y (middle) and I_z (bottom) as a function of frequency before (thin line) and after (thick line) the sensitivity correction ($d=60$ mm, $\delta=0.5$, $\xi=45^\circ$ and $\zeta=0^\circ$, with no phase mismatch).

case, I_x and I_z fluctuate and differ from -2.25 dB because of the phase mismatch. However, both intensities are raised roughly by 0.75 dB after the correction. The errors caused by the phase mismatch still remain in the result but, at least, the sensitivity loss is recovered.

Figure 5 shows the frequency dependence of the effect of sensitivity correction for $d = 60$ mm, $\delta = 0.0$, $\xi = 45^\circ$, $\zeta = 0^\circ$, and with no phase mismatch. The top, middle, and bottom charts are for I_x , I_y , and I_z components, and thin and thick lines are the normalized intensities before and after the correction, respectively. Since the direction of the source is 90° from the y axis, the true value of the normalized y -component intensity is $-\infty$ dB (I_x and I_z components are the same as the previous case). It does not become zero ($-\infty$ in dB) but is given some residual component due to the property of the present 3-D intensity measurement method.²⁾ This component is also reduced by the correction in the frequency range below 2.3 kHz, giving an extra advantage for the proposed method.

Figure 6 shows the frequency dependence of the effect of correction for $d = 60$ mm, $\delta = 0.0$, $\xi = 45^\circ$, $\zeta = 45^\circ$, and with no phase mismatch. The true values are $I_x = I_y = -3.0$ dB and $I_z = -1.5$ dB. Before correction, they have sensitivity reductions of approximately 1 dB at 1.5 kHz. After the correction, the sensitivity errors are within ± 0.3 dB at 2.5 kHz, indicating a significant improvement of the accuracy in the extended range by the proposed method.

Figure 7 shows a result for a case including the phase mismatch among microphones. The phase errors (radian) of microphones 1 to 4 are 0.0 , $+kd/10$, 0.0 , and $-kd/10$, respectively. The phase error of $kd/10$, which equals to 7.6° at 1.2 kHz, is relatively large considering the performance level of currently available instruments. The other simulation conditions are the same as in the case of Fig. 6. Due to the phase mismatch, the measured intensities are not correct even in the low frequency region. However, the sensitivity reduction in the high frequency region is still improved by the proposed method. Figure 7 indicates that the proposed method is robust against the phase mismatch.

Figure 8 shows a result for a case with $\delta = 0.7$. The other conditions are the same as in the case of Fig. 7. The measured intensities are more inaccurate than those in Fig. 7 because of the existence of

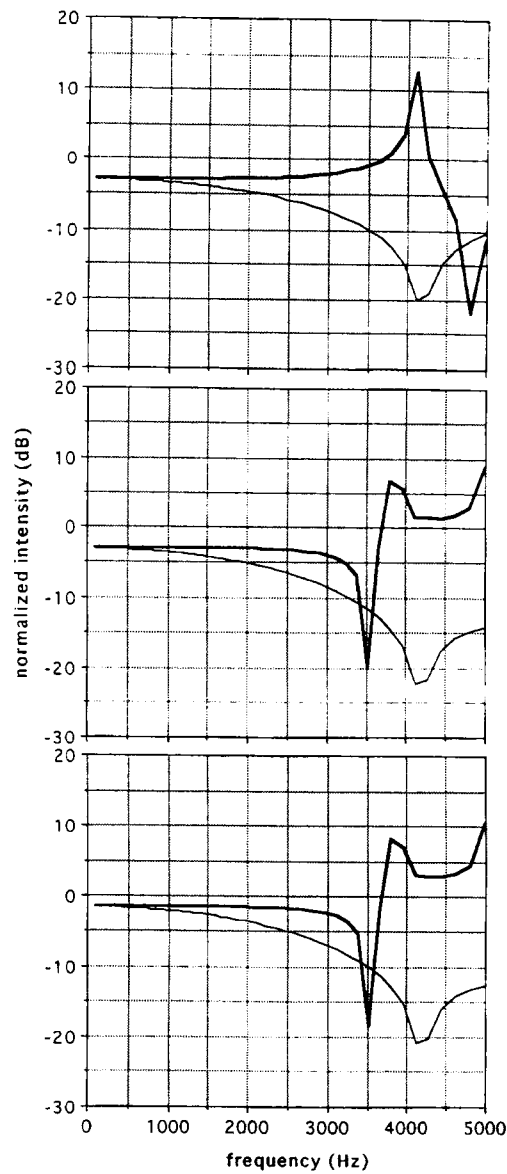


Fig. 6 Normalized intensities I_x (top), I_y (middle) and I_z (bottom) as a function of frequency before (thin line) and after (thick line) the sensitivity correction ($d = 60$ mm, $\delta = 0.0$, $\xi = 45^\circ$, $\zeta = 45^\circ$, and with no phase mismatch).

the reflection. Even in this case, the proposed method reduces the sensitivity reductions of the three intensity components.

If an error of 1 dB is allowed, from numerical simulations for various source directions with no

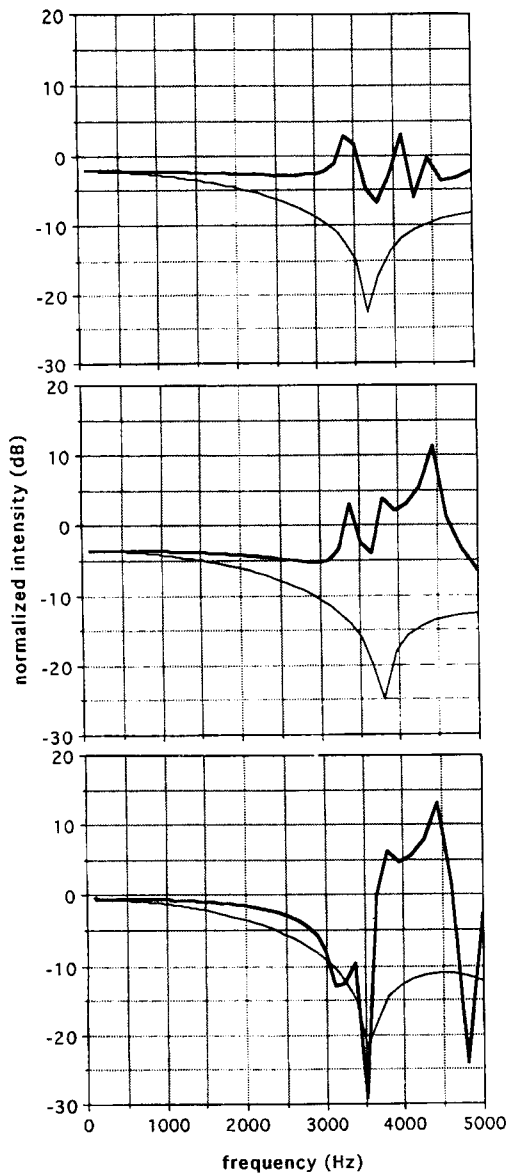


Fig. 7 Normalized intensities I_x (top), I_y (middle) and I_z (bottom) as a function of frequency before (thin line) and after (thick line) the sensitivity correction ($d=60$ mm, $\delta=0.0$, $\xi=45^\circ$, $\zeta=45^\circ$). The phase errors (radian) of microphones 1 to 4 are 0.0, $-kd/10$, 0.0, and $-kd/10$, respectively.

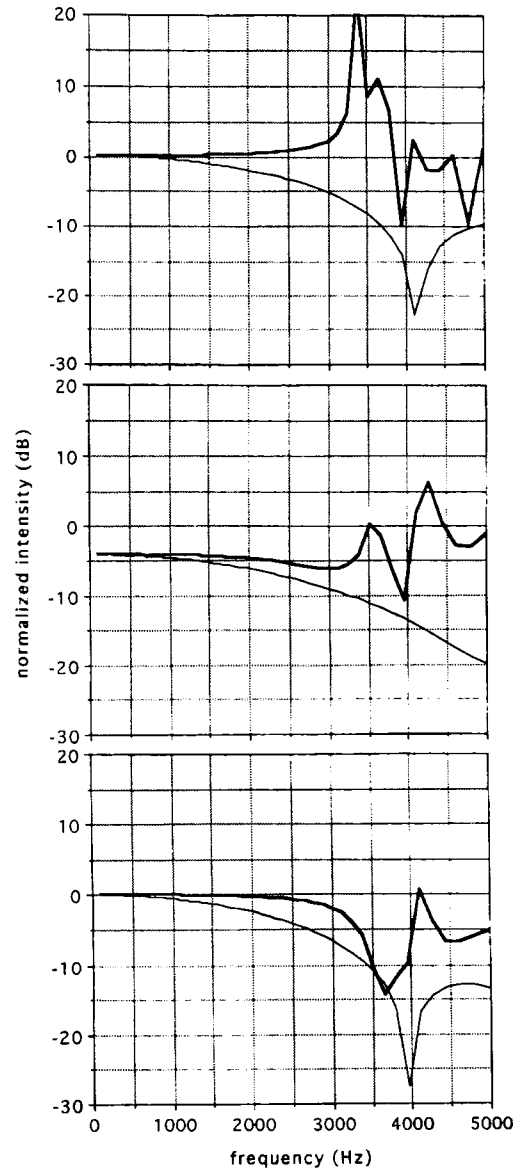


Fig. 8 Normalized intensities I_x (top), I_y (middle) and I_z (bottom) as a function of frequency before (thin line) and after (thick line) the sensitivity correction ($d=60$ mm, $\delta=0.7$, $\xi=45^\circ$, $\zeta=45^\circ$). The phase errors (radian) of microphones 1 to 4 are 0.0, $+kd/10$, 0.0, and $-kd/10$, respectively.

phase mismatch and no reflection, it is known that the 3-D probe of the type shown in Fig. 2 with $d=60$ mm can be used up to 1.3 kHz without the sensitivity correction. From the results given in Fig. 5,

it seems reasonable to say that the same probe, after the sensitivity correction, can be used up to 2.6 kHz at which I_y exceeds the -10 dB level. In the case of Fig. 6, the upper limit frequency is much higher.

6. CONCLUSIONS

A correction method of the sensitivity reduction for a three-dimensional sound intensity probe was presented. The simulation results show that the upper limiting frequency of the 3-D intensity probe can be made approximately two times larger by the proposed sensitivity correction method. This is a significant improvement of the probe performance considering that the microphone separation of the probe can be made two times larger than that of a probe without the sensitivity correction if the same frequency range must be covered. This has the effect of reducing the error due to the phase mismatch in the low frequency range. It also reduces the disturbance of the sound field around each microphones if the microphone separation becomes large.

The simulation results also show that the effect of the proposed method is robust to the phase mismatch among microphones. Since the proposed

method is very general, it can be applied to other types of 3-D intensity probes.^{3,4)}

The simulation was limited to cases where the original and image sources were far from the measurement point. Further simulation studies should be conducted for near-field cases and with multiple sources.

REFERENCES

- 1) F. J. Fahy, *Sound Intensity* (Elsevier Applied Science, London and New York, 1989).
- 2) H. Suzuki, M. Anzai, S. Oguro, and T. Ono, "Performance evaluation of a three dimensional intensity probe," *J. Acoust. Soc. Jpn. (E)* **16**, 233-238 (1995).
- 3) G. Rasmussen, "Measurement of vector sound fields," *Proc. 2nd Int. Congr. Acoustic Intensity*, 53-58 (1985).
- 4) L. M. S. Santos, C. C. Rodoregues, and L. Bento Coelho, "Measuring the three-dimensional acoustic intensity vector with a four-microphone probe," *Proc. Inter-Noise 89*, 965-968 (1989).